




Non-Relativistic Boson Stars as Gravitational Quantum Droplets

Jorge Mastache ^{*}

Consejo Nacional de Ciencia y Tecnología
Av. Insurgentes Sur 1582, Col. Crédito Constructor,
Alc. Benito Juárez, CP 03940. México
Mesoamerican Centre for Theoretical Physics
Universidad Autónoma de Chiapas. Ciudad Universitaria,
Carretera Zapata Km. 4, Real del Bosque (Terán),
29040, Tuxtla Gutiérrez, Chiapas, México

Elías Castellanos [†]

Escuela de Ingeniería y Ciencias
Tecnológico de Monterrey
Carr. Lago de Guadalupe Km. 3.5,
Estado de México 52926, México.

Guillermo Chacón-Acosta [‡]

Departamento de Matemáticas Aplicadas y Sistemas
Universidad Autónoma Metropolitana-Cuajimalpa
Av. Vasco de Quiroga 4871,
Ciudad de México, 05348, México

We analyze the dynamics of a gravitational bounded cloud of generic bosons or a boson star in the non-relativistic regime, assuming from the very beginning that the boson star is in a Bose-Einstein condensed state. Also, we have taken into account multi-particle interactions within the boson star, which are described through the so-called logarithmic potential. Assuming energy conservation conditions at any time, we are able to describe the boson star as a some kind of *gravitational quantum liquid*, or more specifically, as a *macroscopic gravitational quantum droplet*. The assumption of logarithmic interactions, lead us to establish several scenarios in which the system is able to oscillates around the equilibrium radius. The approach analyzed in the present report shows that the interpretation of a boson star as a *macroscopic gravitational quantum droplet* can be applied to the dynamics analysis of a large number of systems on different size scales.

PACS numbers: 95.35.+d, 95.30.Cq, 98.35.Gi, 98.80.Cq, 98.10.+z

1. INTRODUCTION

The relation between Boson Stars (BSs) and galactic dark matter (DM) halos opens up a relevant scheming and a very interesting scenario that deserves deeper analysis despite their lack of detection [1–6]. According to some ideas in the literature, the nature of BSs and DM halos can be understood as some kind of Bose-Einstein condensate made of generic bosons [7–11], although this interpretation depends on the specific model under consideration. BS analysis allows the study of its structural properties, size, and stability, from giant to compact, depending on particle interactions. BSs could appear not only as candidates for dark matter sources but also as mimics of black holes, compact objects formed by axions, and various other astrophysical systems [12]. The commonly employed Gross-Pitaevskii-Poisson approach is valid at very low temperatures and for dilute systems in the non-relativistic regime [13–15]. There is a *zoo* of these objects (BSs) in the literature, basically characterized according to their dynamical

behavior [10]. For instance, BSs could lie in the relativistic regime or not; and they can also be characterized concerning the type of self-interactions within the system [10]. Further possible objects arise when considering rotation [16]. At this point is important to mention that the analysis of more general interactions within the system could lead to new interesting phenomena that can be, in principle, observed.

On the other hand, quantum liquids and the emergence of quantum droplets in Bose-Einstein condensates (BECs) have stimulated several works concerning this fascinating phase transition, for instance, Refs. [17, 21–24]. In the single-component scenario, quantum droplets' formation has also been analyzed, in which three-body and higher-order interactions can be inserted as a logarithmic term in the corresponding interacting potential, for instance. Consequently, it can be proved that the so-called *self-sustainability* or *self-confinement* (that can be interpreted as quantum droplets) emerges [25]. In a recent report [26], it was shown that the inclusion of the so-called logarithmic potential leads to scenarios in which after turning off the corresponding trapping potential, usually described as a first approximation, like a harmonic oscillator potential, the system starts to expand. However, due to the presence of higher-order interactions, the emergence of quantum droplet behavior is reached. In other words, the *self-confinement* or *self-sustainability* for the sin-

*Electronic address: jhmastache@mctp.mx

†Electronic address: elias.castellanos@tec.mx

‡Electronic address: gchacon@cua.uam.mx

gle component system also emerges. Such a connection between quantum liquids and ultracold quantum gases, [17–19], will allow us to interpret BSs as quantum liquids, or more precisely, as *gravitational quantum droplets* composed of generic bosons. In a recent report [20], some structural properties of Non-relativistic Boson Stars (NRBSs) were analyzed under the assumption that the system is in a dynamical equilibrium state. The conditions described in [20] leads us to obtain several gravitational equilibrium configurations, ranging from sizes comparable to compact objects or typical stars to gigantic systems, comparable in size to dark matter halos of galaxy clusters. In this regard, it is essential to mention that in the standard laboratory Bose-Einstein condensates, the trapping potential can be turned off to allow free expansion of the particle cloud. However, it is impossible in the BS gravitational scenario studied in this work since gravity can never be *turned off*. Consequently, we must consider the contributions of the gravitational field upon the BS when calculating the system's ground state energy dynamics. The BSs' behavior in the non-equilibrium dynamical scenario could be more complicated to analyze.

The paper's structure is as follows: Sections 2 and 3 focus on the structural analysis of the NRBS based on a standard solution that includes macroscopic quantities modified by the nonlinear logarithmic potential parameters. Section 4 examines the NRBS parameter space, with an emphasis on attractive interactions, and investigates the nonlinear dynamics of the boson star in response to small perturbations close to the equilibrium case. Finally, the last section provides a brief discussion of the results.

2. NRBS STRUCTURAL EQUILIBRIUM

In order to analyze BS's structural properties and dynamical behavior viewed as *gravitational quantum droplet*, let us define the following energy functional E , associated with the system, namely

$$E = \int d\mathbf{r} \left\{ \frac{\hbar^2}{2m_\phi} |\nabla\Psi|^2 + V(\mathbf{r})|\Psi|^2 + \frac{1}{2}g|\Psi|^4 - \beta|\Psi|^2 \left[\ln(\alpha^3|\Psi|^2) - 1 \right] \right\}, \quad (1)$$

where m_ϕ is the mass of the generic boson, $V(\mathbf{r})$ is the external potential, additionally to the nonlinear logarithmic contribution. Equation (1) defines the energy functional that governs the logarithmic system's properties, as described in Ref. [27]. In Eq. (1), Ψ represents the BEC wave function, also known as the order parameter, the energy of the ground state of the N -particle system. The introduction of the logarithmic potential in nonlinear quantum mechanics has interesting implications [28]. It is the only case where the subsystems can be separable, i.e., no correlations are induced. This potential also has interesting features, such as a lower energy limit and the occurrence of soliton-like traveling wave solutions. These features are crucial for defining localized macroscopic objects. In the case of the Schrödinger equation, one

can establish bounds for the logarithm parameter using high-precision measurements in atomic physics. Different kind of experiments may help to impose such bounds in the case of the equation for the order parameter (see [26]).

On the other hand, in Ref. [20] the suggested approximation for the gravitational contribution can be written as

$$V(r) = \frac{1}{2}m_\phi\omega_g^2r^2, \quad (2)$$

i.e., as a trapping harmonic-like potential, where

$$\omega_g^2 = \gamma\pi Gm_\phi N\rho(r \approx 0), \quad (3)$$

is defined as an *effective gravitational frequency*, together with $\rho(r \approx 0)$, the central density of the NRBS. Notice that we have included in the *effective gravitational frequency* the parameter γ , which is related to the regime of validity of the approximation; see Ref. [20] and references therein for details. Additionally, $g = 4\pi\hbar^2 a/m_\phi$ is the interaction strength between any pair of bosons, with the s-wave scattering length a of the corresponding system, N is the number of particles, while β and α^3 measure the strength of the nonlinear logarithmic interaction.

In order to calculate the ground state energy associated with the energy functional Eq. (1), we have to formally solve the corresponding equation of motion. However, to simplify the calculations, we can employ an accurate expression for the total energy of the cloud that can be obtained by using an *ansatz* of the form [29, 30]

$$\psi(r) = \frac{N^{1/2}}{\pi^{3/4}R^{3/2}} e^{(-r^2/2R^2)} e^{i\varphi(r)}, \quad (4)$$

The gaussian *ansatz* above corresponds to the solution of the Schrödinger equation in the non-interacting regime, with N the number of particles within the NRBS. Note that $e^{i\varphi(r)}$ is a phase factor that involves particle currents [29]. Additionally, we interpret the length $R^2 = \hbar/m\omega_g$ as the initial size of the NRBS in the ideal (non-interacting) case, i.e., when $g = \beta = 0$. Thus, by inserting the gaussian *ansatz* (4) in the energy functional Eq. (1) we obtain the ground state energy, given by

$$E = E_k + E_p, \quad (5)$$

where E_k is the kinetic energy associated with particle currents [29]

$$E_k = \frac{\hbar^2}{2m_\phi} \int d\mathbf{r} |\psi(\mathbf{r})|^2 (\nabla\varphi(\mathbf{r}))^2. \quad (6)$$

On the other hand, E_p can be interpreted as the energy associated with an effective potential, which is equal to the total energy of the condensate when the phase φ does not vary in space. The term E_p contains the contributions of the zero point energy E_0 , the *effective gravitational potential* (E_{pot}), and the contributions due to the interactions among the particles within the condensate (E_{int}), namely

$$E_p = E_0 + E_{pot} + E_{int}, \quad (7)$$

where

$$E_0 = \frac{\hbar^2}{2m_\phi} \int d\mathbf{r} \left| \frac{d\psi(\mathbf{r})}{dr} \right|^2, \quad (8)$$

$$E_{pot} = \frac{1}{2} m_\phi \omega_g^2 \int d\mathbf{r} r^2 |\psi(\mathbf{r})|^2, \quad (9)$$

$$E_{int} = \frac{1}{2} g \int d\mathbf{r} |\psi(\mathbf{r})|^4 \quad (10)$$

$$- \beta \int d\mathbf{r} |\psi(\mathbf{r})|^2 \left[\ln(\alpha^3 |\psi(\mathbf{r})|^2) - 1 \right],$$

Consequently, E_p can be written as follows

$$E_p = \frac{3\hbar^2 N}{4m_\phi R^2} + \frac{3m_\phi \omega_g^2 R^2 N}{4} + \frac{g N^2}{4\sqrt{2\pi} R^3} \quad (11)$$

$$- \beta \left(\frac{3\sqrt{\pi}}{2} \ln \left(\frac{\alpha^3 N}{R^3} \right) + c \right) N,$$

where $c = \frac{3\sqrt{\pi}}{2} \ln \pi + 14\sqrt{\pi}$ is an irrelevant constant when energy conservation conditions are assumed in the system.

The equilibrium radius of the system R_0 , can be calculated by minimizing the energy E_p in Eq. (5), that is, $dE_p/dR|_{R=R_0} = 0$. We must mention here that the parameter R_0 can be related to the standard size of the NRBS (at, let's say, time $t = t_0$, or equivalently, at the equilibrium radius). In addition, the so-called R_{99} , is an effective radius defining a spherical surface within which the 99% of the star's mass is enclosed. Furthermore, the ratio between R_{99} and R_0 is a fixed value $\kappa = (R_{99}/R_0)$ which depends on the chosen *ansatz*. In the case of the gaussian *ansatz*, κ is of order 2.8, [20, 30].

The corresponding pressure is calculated using the standard definition $P = -(\partial E_p / \partial V_{eq})$, where $V_{eq} = 4\pi\kappa^3 R_0^3 / 3$ see [20], leading to the result:

$$P_{(0)} = \left(\frac{3}{4\pi^{1/4}} \right)^{2/3} \frac{\gamma G \kappa m_\phi^2 N^2}{3V_{eq}^{4/3}} + \sqrt{\frac{\pi}{2}} \frac{g \kappa^3 N^2}{3V_{eq}^2} \quad (12)$$

$$+ \left(\frac{3\pi^2}{4} \right)^{1/3} \frac{2\hbar^2 \kappa^2 N}{3m_\phi V_{eq}^{5/3}} - \frac{3}{2} \frac{\sqrt{\pi} \beta N}{V_{eq}}.$$

It is quite interesting to analyze the corresponding equation of state (EoS) for several regimes [20]. Let us consider, for instance, the following two regimes: on the one hand, the ideal case where $g = \beta = 0$, and on the other hand, at zero temperature. In the first case, we obtain $P_{(0)} = 2/3(E_p/V_{eq}) = (2/3)\rho_\epsilon$, i.e., the EoS for an ideal non-relativistic gas. When the temperature $T \rightarrow 0$ and interactions are neglected, we obtain the pressure $P_{(0)} \rightarrow 0$, i.e., *dust*. We can also obtain a *stiff matter*-like EoS when the temperature $T \rightarrow 0$ and the pair interactions dominate the system $g \gg \beta$; in other words, $P_{(0)} = E_p/V_{eq} = \rho_\epsilon$, the pressure is proportional to the energy density ρ_ϵ when $T \rightarrow 0$.

3. NRBS STRUCTURAL DYNAMICS

Let us now analyze the dynamics of the NRBS when seen as a *gravitational quantum droplet*. For this purpose, we calculate the kinetic energy contributions Eq. (6). Remark that Eq. (6) is positive definite and is zero when the phase $\varphi(r)$ is constant [29]. Thus, the corresponding motion of the condensate corresponds to potential flow since the velocity is the gradient of the scalar quantity $\varphi(r)$, referred to as the velocity potential. By changing R from its initial value to a new value \bar{R} , amounts to a uniform dilation of the system since the new density distribution $|\psi(r)|^2$ may be obtained from the previous one by changing the coordinate of each particle by a factor \bar{R}/R [29]. Then, the velocity of a particle is given by

$$v(r) = r \frac{\dot{R}}{R}. \quad (13)$$

Thus, it is straightforward to obtain the kinetic energy E_k by using the *ansatz* Eq. (4), yielding

$$E_F = \frac{3Nm_\phi}{4} \dot{R}^2. \quad (14)$$

With the assumption of energy conservation conditions at any time, we obtain the following energy conservation condition associated with the cloud or the NRBS at any time

$$\frac{3Nm_\phi}{4} \dot{R}^2 + \frac{3\hbar^2 N}{4m_\phi R^2} + \frac{3m_\phi \omega_g^2 R^2 N}{4} + \frac{g N^2}{4\sqrt{2\pi} R^3}$$

$$- \beta \left(\frac{3\sqrt{\pi}}{2} \ln \left(\frac{\alpha^3 N}{R^3} \right) \right) N$$

$$= \frac{3\hbar^2 N}{4m_\phi R_0^2} + \frac{3m_\phi \omega_g^2 R_0^2 N}{4} + \frac{g N^2}{4\sqrt{2\pi} R_0^3} \quad (15)$$

$$- \beta \left(\frac{3\sqrt{\pi}}{2} \ln \left(\frac{\alpha^3 N}{R_0^3} \right) \right) N,$$

where R_0 is the equilibrium radius of the NRBS at, let say, time $t = t_0 = 0$, and R is function of time and corresponds to the radius at time t . It is important to mention here that when the ground state pressure dominates over gravity and the contribution of interactions, an analytical solution can be obtained for Eq. (15), giving

$$R(t)^2 = R_0^2 + (v_0 t)^2 \quad (16)$$

where v_0 can be interpreted as *free velocity expansion* of the cloud, corresponding to the velocity predicted by Heisenberg's uncertainty principle for a particle confined to a distance R_0 . Clearly, under more general conditions, i.e., for relevant contributions of g and β together with representative gravity contributions, the dynamical structural properties of the NRBS must be modified, as we will see later in following sections.

4. NUMERICAL ANALYSIS OF NRBS DYNAMICS

We study the parameter space defined by the mass, m_ϕ , the s -wave scattering length, a , the number of particles, N , and

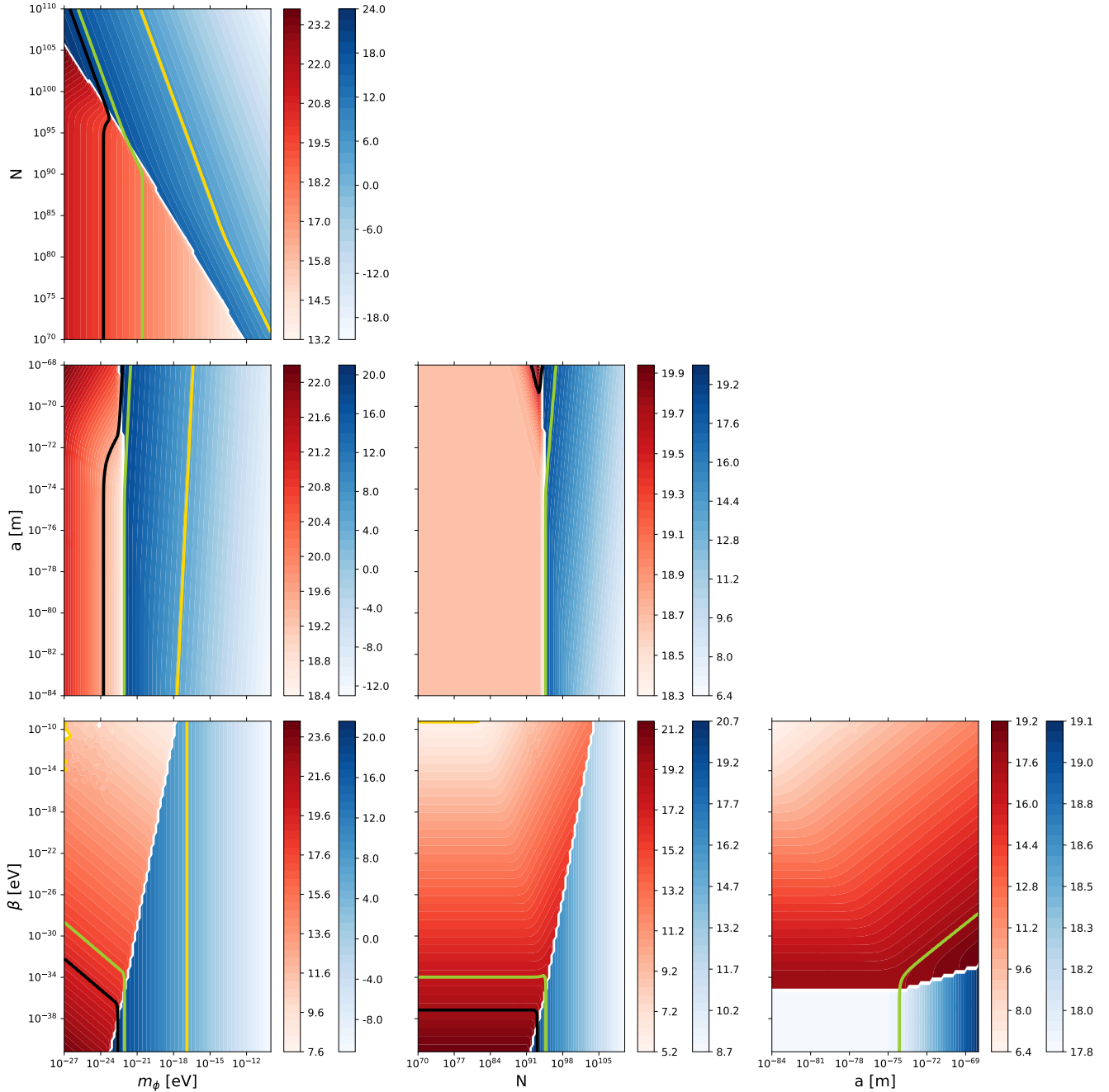


FIG. 1: Triangular plot of the parameter space for a quantum-droplet model, with parameters m_ϕ , a , N , and β fixed to the benchmark values for the Dwarf DM halo system shown in Table I. The specific values for the non-linear interactions are for $\beta > 0$. The yellow, green, and black lines correspond to isolines for systems with radii similar to the Sun, a Dwarf DM halo, and a Galaxy cluster DM halo, respectively. The intensity of the color corresponds to the radii values, $\log_{10}(R_0/\text{km})$, with red regions representing areas where the non-linear interaction of the particles dominates. In contrast, regions in blue indicate systems where gravitational and quantum interactions dominate.

the β and α , which measure the strength of a nonlinear logarithmic interaction, i.e., a many-body interaction. In this study, we use the bounds for m_ϕ , a , and N given in a previous work [20] as a preliminary framework for establishing the parameter space of interest and defining it as our benchmark systems. However, these bounds are not applied stringently in our anal-

ysis but are used to guide the scaling. Specifically, we expand the upper bounds and reduce the lower bounds by one order of magnitude. This adjustment allows us to investigate a broader range of conditions while referencing previous benchmarks. The β parameter, which will be clear in the analysis below, should have a range close to m_ϕ so the logarithmic interac-

| | m_ϕ [eV] | N | a [m] | β [eV] | R_0/R_i | E/E_{Roi} |
|---------------------------|------------------------|------------------------|------------------------|------------------------|-----------|-------------|
| Sun ^{min} | 1.51×10^{-14} | 3.84×10^{82} | 7.33×10^{-73} | 1.47×10^{-18} | 1.03 | 0.01 |
| Sun | 1.23×10^{-12} | 5.52×10^{76} | 1.00×10^{-68} | 4.23×10^{-35} | 0.61 | 1.74 |
| Sun ^{max} | 4.15×10^{-11} | 6.28×10^{71} | 7.92×10^{-84} | 6.24×10^{-42} | 0.97 | 2.00 |
| Dwarf DM ^{min} | 1.30×10^{-21} | 3.74×10^{91} | 6.96×10^{-71} | 3.53×10^{-36} | 0.99 | 0.01 |
| Dwarf DM | 9.25×10^{-23} | 5.24×10^{94} | 7.72×10^{-75} | 3.53×10^{-36} | 1.29 | 0.72 |
| Dwarf DM ^{max} | 4.26×10^{-24} | 5.81×10^{98} | 1.00×10^{-84} | 6.24×10^{-42} | 0.99 | 2.00 |
| Dwarft DM ^{ref} | 2.34×10^{-22} | 1.44×10^{93} | 4.28×10^{-72} | 7.05×10^{-37} | 3.9 | 0.22 |
| Cluster DM ^{min} | 4.72×10^{-25} | 8.13×10^{101} | 1.11×10^{-72} | 2.40×10^{-29} | 1.04 | 0.01 |
| Cluster DM | 1.40×10^{-26} | 4.04×10^{104} | 6.28×10^{-83} | 1.85×10^{-35} | 1.14 | 0.60 |
| Cluster DM ^{max} | 3.04×10^{-25} | 3.65×10^{100} | 1.00×10^{-84} | 6.24×10^{-42} | 0.95 | 2.00 |

TABLE I: Parameters for different objects with positive β . Parameter space for different astrophysical systems modeled as gravitational quantum droplets with a positive nonlinear interaction strength ($\beta > 0$). The table shows the scalar field mass m_ϕ , number of particles N , s-wave scattering length a , nonlinear interaction strength β , the ratio of equilibrium radius R_0 to reference radius R_i , and the ratio of total energy E to reference energy E_{0i} for i -systems analogous to the Sun, a Dwarf DM halo, and a DM Cluster halo in their minimum positive energy state (^{min}), the closest to the benchmark system, and maximum energy state (^{max}). We also present our reference system (^{ref}) for which we use it as an example to compute the evolution of the system.

tion remains relevant. The parameter α is initially set to one since it will only change the energy of the system, but it does not affect the evolution.

As we mentioned above, the equilibrium radius, R_0 , of the system is determined by finding the radius at which $dE_p/dR|_{R=R_0} = 0$, where E_p is defined in Eq. (7). We need to find the real and positive roots of the polynomial

$$1 - \frac{A}{R_0^4} - \frac{B}{R_0^5} + \frac{C}{R_0^2} = 0 \quad (17)$$

to find R_0 . In the last expression, we have used the following definitions

$$A = \frac{\hbar^2}{m^2\omega_g^2}; \quad B = \frac{gN}{4m\omega_g^2} \sqrt{\frac{2}{\pi}}; \quad C = \frac{3\sqrt{\pi}\beta}{m\omega_g^2}.$$

Notice that R_0 does not directly depend on the parameter α value. A is related to the zero-point energy state, indicating smaller-scale quantum fluctuations. The coefficient B quantifies the s-wave scattering interaction energy among the bosons directly resulting from their mutual contact interactions. The term involving C introduces corrections from both logarithmic and linear terms to the interaction dynamics between particles.

The relationships $B/A = \sqrt{2\pi}(aN)$ and $C/A = 3\sqrt{\pi}/\hbar^2(m\beta)$ shows the degeneracy of the parameters within the system. Adjustments in others could offset variations in one parameter. This degeneracy suggests an interdependence between the physical constants and the interaction parameters, complicating the individual effects without thoroughly exploring the entire parameter space. Moreover, we explore positive and negative values for β , leading to different system evolution in each case.

We present a comprehensive parameter space analysis in Figure 1. First, let us analyze the case in which $\beta > 0$; in subsection 4.1, we will present the case for $\beta < 0$. We show a triangular plot with the contour plots for each parameter

(m_ϕ , a , N , and β) against the others, revealing the correlations within the parameter space. For each contour plot, we marginalize the parameters for the benchmark system values for the Dwarft DM halo system as shown in Table I. The yellow, green, and black lines correspond to isolines for systems with radii comparable to the Sun ($R_0 = R_\odot = 6.96 \times 10^5$ km), a DM halo of a Dwarf galaxy ($R_0 = 22$ kpc), and a galaxy cluster DM halo ($R_0 = 10^3$ kpc), respectively. The color intensity within the contours corresponds to the values of $\log_{10}(R_0/\text{km})$. The regions shaded in red represent areas of the parameter space where the non-linear interaction of the particle dominates, implying a stronger contribution from the logarithmic interaction term. In contrast, regions shaded in blue indicate systems where gravitational and quantum pressure effects dominate, minimizing the influence of the non-linear interactions. These color-coded zones help distinguish between regimes governed by different physical processes within the framework of a quantum droplet. In appendix A, we show triangular plots with the parameter space marginalized in Sun-like systems and Cluster DM halo systems.

Upon determining the equilibrium radius R_0 , we analyze the energy given by Eq.(11), and the temporal evolution of R by solving Eq.(15). The dimensionless form for the energy is given by

$$\frac{E}{E_{Ro}} = x^2 + \frac{A}{R_0^4} \frac{1}{x^2} + \frac{2}{3} \frac{B}{R_0^5} \frac{1}{x^3} - \frac{4k}{9\sqrt{\pi}} \frac{C}{R_0^2} - 2 \frac{C}{R_0^2} \ln \left(\frac{\alpha N^{1/3}}{x R_0} \right), \quad (18)$$

where $x = R/R_0$ and E_{Ro} is a reference energy for the system defined by $E_{Ro} \equiv \frac{3}{4} m_\phi N \omega_g^2 R_0^2$. The evolution in its dimen-

sionless form is given by

$$\left(\frac{dx}{dy}\right)^2 = (1-x^2) + \frac{A}{R_0^4} \left(1 - \frac{1}{x^2}\right) + \frac{2B}{3R_0^5} \left(1 - \frac{1}{x^3}\right) - \frac{2C}{R_0^2} \ln x, \quad (19)$$

with $y = \omega_g t$. Notably, the parameter α does not influence either the size of the system, R_0 , or the evolution of $x(y)$, indicating its role is constrained to scaling the nonlinear interaction energy of the system and, for this reason, it is not considered as a free parameter and its value is set to $\alpha = 1$.

The solution of the differential equation (19) uniquely indicates that the state remains at the equilibrium, $x = 1$, for all times under the assumptions of perfect system isolation. This is, the system for one set of parameters m_ϕ , N , a , and β defines a radius R_0 , and no other real, positive solution for x exists.

The system is a gravitationally bound cloud described as a boson star in the non-relativistic limit that we interpreted as a *gravitational quantum droplet*. Its energy depends on the Bose-Einstein zero-energy state and the multi-particle interactions, characterized by a logarithmic potential. The energy equation shows that systems at equilibrium can have total negative energy. Such a condition is achieved when the interaction energy predominates over the zero-point energy (E_0) and the confining harmonic-like potential energy (E_{pot}). Negative total energy indicates a stable, bound state where the attractive interactions lead to a net energy reduction sufficient to bind the system against external perturbations. These bounded states in which the interactions dominate appear in red in the parameter space as in Fig. 1.

An example of negative total energy is observed in ${}^7\text{Li}$ BECs, where inter-atomic forces via Feshbach resonances allow experimentalists to toggle the interaction from repulsive to attractive, leading to interesting phenomena like the formation of bright solitons and the potential for collapse (or Bosenova) when the attractive forces overpower the system's stability mechanisms [32]. Analogous processes may occur in the gravitational quantum droplets.

We can better understand the energy at the equilibrium by substituting the constriction given by Eq.(17) into Eq.(18), this gives

$$\frac{E}{E_{Ro}} \simeq 2 - \frac{1}{3} \frac{B}{R_0^5} - \frac{2C}{R_0^2} \left(3 + \ln \left[\frac{\alpha N^{1/3}}{R_0} \right] \right) \quad (20)$$

for positive values of β , C is positive; the maximum value of the energy is reached when B/R_0^5 and C/R_0^2 do not contribute to the energy system; this is, the states with maximum energy are given by the smallest values for the scattering s-wavelength a and smallest values of β . Therefore, the maximum value is $E/E_{Ro} \simeq 2$ as shown in Table I, which summarizes the parameters describing quantum droplets with similar sizes of various astrophysical systems with a positive nonlinear logarithmic interaction strength, β . The systems studied include configurations analogous to the Sun, the DM halo of a dwarf galaxy, and the DM halo of a galaxy cluster. For each

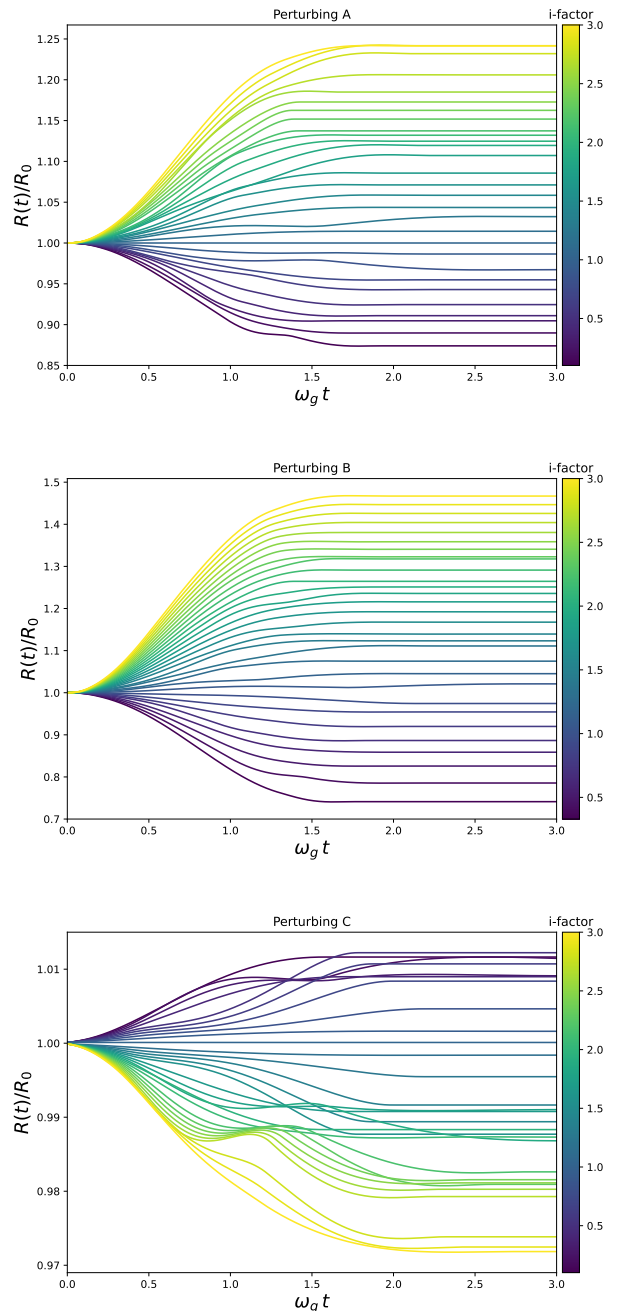


FIG. 2: Plot of the evolution of a boson star given by Eq.(19), for values of B that deviate from the equilibrium state. Smaller values, B/i , are shown in the top panel, and larger values, $B \cdot i$, in the bottom panel. The i -factor is indicated on the color bar.

system, three configurations are explored: one corresponding to the minimum positive energy state (denoted by $^{\min}$), the benchmark reference system (no superindex), and a configuration with maximum energy (denoted by $^{\max}$). When exploring the parameter space to find the system with maximum and minimum energy, we take a 5% tolerance in the value or the radius of interest. The Sun-like systems show increasing com-

compactness and energy as we progress from the minimum to the maximum energy states.

The ultra-light DM model, also known as fuzzy-DM, particularly with a scalar field mass around $m_\phi \sim 10^{-21}$ eV, has been a compelling candidate in recent years. This model suggests that dark matter could be composed of extremely light bosons, resulting in a de-Broglie wavelength large enough to prevent the formation of small-scale structures. Our findings around the Dwarf DM system align well with previous results, particularly for $\beta > 0$, see Table I, where we obtained a mass $m_\phi \sim 1.3 \times 10^{-21}$ eV, close to the expected range for ULDM [31].

Now, we consider perturbing the initial state, changing the value of one of the parameters while maintaining the others at a fixed value, to understand the system and explore its stability and response. Considering a deviation from the number of particles that maintains the system in dynamical equilibrium, N , directly affects the value of B . And it can indirectly influence A and C under their dependence of N through ω_g ; we study scenarios where A , B , and C change independently to gain deeper insights into the system out of equilibrium.

Figure 2 presents the solutions of Eq. 19 for various perturbed values of A , B , and C , illustrating the system behavior when it deviates from its initial state set to $R = R_0$. Each line in the figure represents a solution of Eq. (19) with a deviation quantified by i -factor, which drives the system away from R_0 . The system can rapidly expand or contract, depending on whether we inject or subtract energy from the system; for instance, increasing the value of A will be equivalent to injecting energy into the system, making it expand to find a larger equilibrium radius. However, increasing C would reduce the energy, analogous to having stronger non-linear interactions, making the system contract. When the system expands, we use the positive solution from the square root in Eq.(19); conversely, when the system contracts, we use the negative solution from the square root. Such observations are essential for understanding the stability characteristics of the system.

Notice that when particle interactions are negligible, $\beta \rightarrow 0$ and $U_0 \rightarrow 0$, together with a weak gravitational interaction, we can analytically integrate Eq.(19) and recover the free expansion

$$x^2 = 1 + \frac{A}{R_0^4} y^2 \quad (21)$$

$$= 1 + \frac{v_0^2}{\omega_g^2 R_0^2} y^2, \quad (22)$$

where $v_0 \equiv \hbar/mR_0$ is the velocity of a free expanding ideal gas. Remembering the definition of y the quantity $y/\omega_g = t$.

A with gravitational bounded system with $\beta \rightarrow 0$ and $U_0 \rightarrow 0$, lead us to the following behaviour

$$x^2 = 1 + \left(\frac{A}{R_0^4} - 1 \right) \sin^2(y) \quad (23)$$

$$= 1 + \left(\frac{v_0^2}{\omega_g^2 R_0^2} - 1 \right) \sin^2(y). \quad (24)$$

The quantity $\omega_g R_0$ can be interpreted as the compactness of the system in the sense that a large value suggests that the

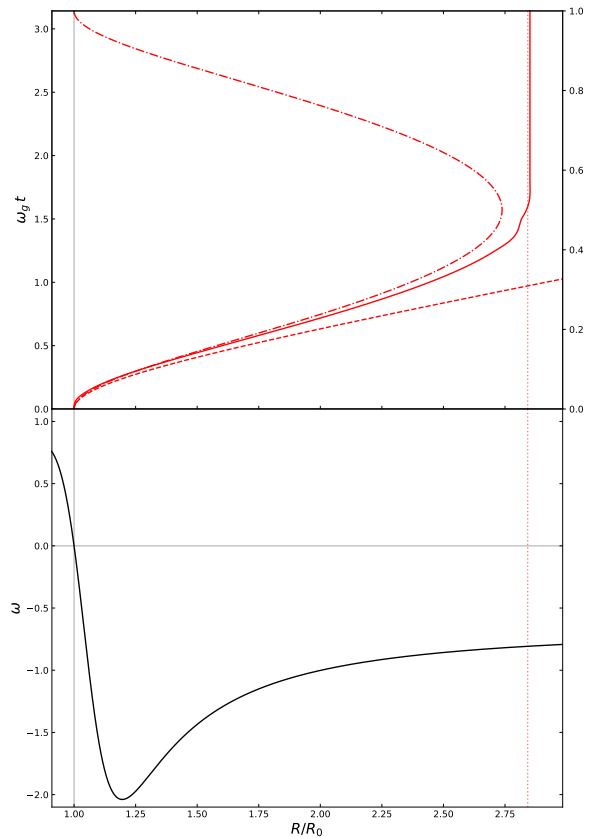


FIG. 3: **Top panel:** The evolution of a the Dwarf DM halo system perturbing $A \rightarrow 50A$. The red dashed is the evolution of an ideal free-expanding gas; The dot-dashed red line is the expansion of an only-gravitation bounded system. The red solid line is the evolution of a gravitational quantum droplet given by the solution of Eq.(19). **Bottom panel:** The equation of state of the unperturbed system. The vertical dotted red line in both panels is the new equilibrium radii, computed using Eq.(17).

gravitational potential is deep and the oscillations of the system are significant. In contrast, a small value might indicate a less dense or weak gravitational configuration. If $v_0 \gg \omega_g R_0$ the system expands and for small times, $y \rightarrow 0$, we recover Eq.(21). In contrast, if $v_0 \ll \omega_g R_0$ gravity overtakes the expansion and the system collapses.

In Fig. 3, we present the solutions for three cases: the free expansion (Eq.(21)), the only-gravitationally bound system (Eq.(23)), and the gravitational quantum droplet (Eq.(19)). The plot corresponds to a configuration resembling a DM halo of a Dwarf galaxy, where the condition $A/R_0^4 \sim 2B/3R_0^5 \sim 2C/R_0^2$ holds. This setup represents our reference system, as detailed in Table I. To explore the dynamics, we introduce a perturbation to the parameter A as $A \rightarrow \xi A = 50A$, where ξ is the magnitude of the perturbation. A large value of ξ is used in this case to highlight the differences between the free expansion solution and the solution for a only-gravitationally bound system. Following this perturbation, energy is artificially injected into the system, causing it to expand until gravitational forces halt the expansion at the characteristic time

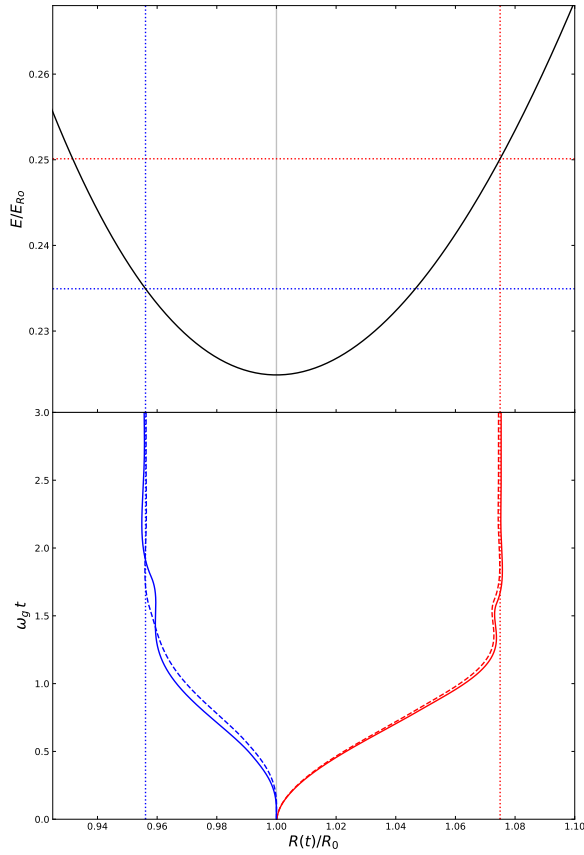


FIG. 4: Top panel: Initial energy value for the perturbed states. Bottom panel: The evolution of the system when it is expanding is in red, and when it is contracting, it is in blue. Solid color lines is for positive β , while dashed color lines are for the same value of β but negative. Vertical dotted lines are defined by their energy limit.

$\omega_g t \approx \pi/2$. This is a characteristic timescale that is a common feature for different configurations. In the case of the only-gravitationally bound system without quantum effects, it contracts after the initial expansion and keeps oscillating. In contrast, the gravitational quantum droplet reaches a new equilibrium radius more quickly, indicating that non-linear particle interactions play a critical role in stabilizing the system. Some oscillations are observed before the system settles into this new equilibrium state. The new equilibrium radius, R'_0 , can be calculated using Eq. (17), by adjusting the parameters to $A \rightarrow \xi A$ and $R_0 \rightarrow R'_0$ to account for the perturbation.

Now, we compute the pressure given by $P = -dE/dV$. We first define the volume as $V = \frac{4}{3}\pi(\kappa R)^3$, and $V_0 \equiv V(R_0)$. Therefore, deriving Eq.(18) gives

$$\frac{P}{P_0} = -\frac{2}{3} \left(\frac{V_0}{V}\right)^{1/3} + \frac{2A}{3R_0^4} \left(\frac{V_0}{V}\right)^{5/3} + \frac{2B}{3R_0^5} \left(\frac{V_0}{V}\right)^2 - \frac{2C}{3R_0^2} \frac{V_0}{V}, \quad (25)$$

where $P_0 = E_{R_0}/V_0$. Using the fact that $x = (V/V_0)^{1/3}$, the

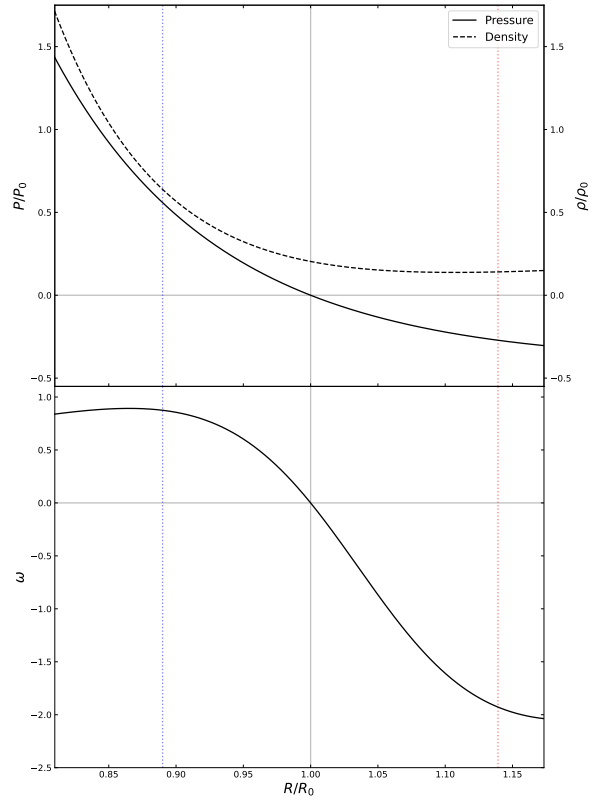


FIG. 5: Top panel: The straight and dotted lines depict the pressure and energy density of the system, respectively. Bottom panel: Is the equation of state $\omega = P/\rho_e$. Vertical dotted lines are defined by their energy limit.

last equation can be written as,

$$\begin{aligned} \frac{P}{P_0} &= -\frac{2}{3} \frac{1}{x} + \frac{2A}{3R_0^4} \frac{1}{x^5} + \frac{2B}{3R_0^5} \frac{1}{x^6} - \frac{2C}{3R_0^2} \frac{1}{x^3} \quad (26) \\ &= -\frac{2}{3} \frac{R_0}{R} \left(1 - \frac{A}{R^4} - \frac{B}{R^5} + \frac{C}{R^2}\right). \quad (27) \end{aligned}$$

In the range $x < 1$, the system can be under compression, and it experiences compressive forces among its constituents. We could also have negative pressure for $x > 1$, where the repulsive interactions of the systems dominate and exert a repulsive force in the star until it reaches equilibrium with the gravitational force. The term in parenthesis is Eq.(17), which implies that at $R = R_0$, or $x = 1$, we have a pressureless system, $P = 0$ because the system is perfectly balanced.

We now could defined the energy density as $\rho = E/V$, then we can write Eq.(18) as

$$\frac{\rho}{\rho_0} = \frac{1}{x} + \frac{A}{R_0^4} \frac{1}{x^5} + \frac{2}{3} \frac{B}{R_0^5} \frac{1}{x^8} - 2 \frac{C}{R_0^2} \frac{1}{x^3} \left(\frac{2k}{9\sqrt{\pi}} + \log \left(\frac{\alpha N^{1/3}}{x R_0} \right) \right) \quad (28)$$

where $\rho_0 = E_{R_0}/V_0$.

Figs. 4 and 5 show the perturbation ($A \rightarrow \xi A$) of the reference Dwarf system under expansion (in red) for $\xi \approx 2.25$, and under compression (in blue) for $\xi \approx 0.29$, for positive values of β (solid lines), and negative values of β (dashed lines)

in the bottom panel of Fig.4. The pressure (Eq.(26)) and energy density (Eq.(28)) is shown in the top panel of Fig. 5 with its corresponding equation of state, $\omega = P/\rho$, in the bottom panel.

Let us summarize what occurs when perturbing a system initially at equilibrium, with its energy ratio $E(x = 1, A, B, C, R_0)/E_{R_0}$ given by Eq.(18). Perturbing the system involves changing one of the parameters while marginalizing the others. The energy of the system increases for perturbations where $\xi > 1$ and $A \rightarrow \xi A$. As a result, the system is no longer in a stable configuration and will experience repulsive pressure due to the zero-point energy of quantum fluctuations. This causes the system to expand with an initial free expansion velocity, lasting for a period given by $\omega_g t \approx \pi/2$. As the system expands, gravitational forces eventually slow down the expansion and attempt to cause the system to contract. However, the non-linear interactions prevent a complete collapse, leading to oscillations around a new equilibrium radius before reaching equilibrium at R'_0 . The system's energy at this new equilibrium, $E'(x = R'_0/R_0, \xi A, B, C, R_0)/E_{R_0}$, is equivalent to $E'(x = 1, \xi A, B, C, R'_0)/E_{R'_0}$, where $E_{R'_0}$ is the reference energy of the system at R'_0 . The following relationship for the energy can then be derived.

$$\frac{E'}{E_{R'_0}} = \left(\frac{R_0}{R'_0}\right)^2 \frac{E'}{E_{R_0}} \quad (29)$$

4.1. Case for $\beta < 0$.

Table II presents the same astrophysical systems (Sun-like, Dwarf DM, and Cluster DM), but now with a negative non-linear interaction coefficient, $\beta < 0$. As in Table I, we explore three configurations for each system: minimum energy (^{min}), the benchmark reference, and maximum energy (^{max}). With negative β the systems exhibit significantly higher energy states compared to their positive β counterparts.

When $\beta < 0$, the maximum value for the energy of the system is not constricted since the last term in Eq.(20) goes as $\ln N$. However, the minimum value of the energy is given when C/R_0^2 is minimum and $B/R_0^5 \rightarrow 1$ hence the minimum value for the energy is $E/E_0 \simeq 5/3 \approx 1.67$, this can also be noticed in Table II for systems with the minimum energy.

If $\beta < 0$, then $C < 0$, but the system can still be dominated by non-linear particle interactions, in particular due to the logarithmic term in Eq.(18). If $\frac{2k}{9\sqrt{\pi}} - \log\left[\frac{\alpha N^{1/3}}{x R_0}\right] < 0$, the system is still dominated by particle interactions independent of A, B , and C . This implies that if

$$\alpha < \frac{R_0 x}{N^{1/3}} e^{-\frac{2k}{9\sqrt{\pi}}} \approx 0.03 \frac{R_0}{N^{1/3}} \quad (30)$$

for the last expression, we use $x = 1$. Additionally, this implies a threshold limit for the number of particles

$$N < 2.8 \times 10^{-5} \left(\frac{x R_0}{\alpha}\right)^3, \quad (31)$$

or for the equilibrium radius

$$R_0 < 32.88 \left(\frac{\alpha N^{1/3}}{x}\right). \quad (32)$$

We plot the isoline of the last expression in Fig.6 in magenta, which is a good approximation for the border between systems dominated by particle interactions.

5. CONCLUSIONS

This paper analyzes non-relativistic boson stars (NRBS), focusing on the nonlinear logarithmic potential and its implications over the system dynamics. Boson stars, understood as generic gravitational BECs, have been used to explore their relationships with dark matter halos and also with their stability. Our study reveals that NRBS can be effectively described as *gravitational quantum droplets* which is remarkable, providing a self-sustaining model applicable to a wide range of scales, ranging from star-sized objects to galactic halos. Stable solutions were found under non-perturbative conditions, resulting in the behavior of the system being strongly influenced by the parameters of the inter-particle interactions and the nonlinear potential. Noteworthy is the oscillatory response of the system to small perturbations near the equilibrium radius. The results provide a solid framework for understanding the structural and dynamical properties of NRBS in both equilibrium and quasi-equilibrium situations, that in principle, could lead to more critical scenarios out of the equilibrium, i.e., explosions and/or implosions and meta-stable configurations. In other words, given that when logarithmic interactions exist, it is very interesting to study *bosenova-like effects* and collapse, clearly within the region of validity for our model. Finally, in future works we will study the dynamics for more general and complicated situations, i.e., gravitational collapse, or explosions, the of *gravitational quantum droplet* under rotation, the eventual case of ejection of matter in the form of JETS and the extension to the semi-relativistic and total relativistic regimes, and also the eventual application to dark matter halos in the form of *gravitational quantum droplets*.

[1] S. J. Sin, Phys. Rev. D 50 (1994) 3650.

[2] F. S. Guzmán, T. Matos and H. Villegas, Astron. Nachr. 320 (1999) 97.

[3] F. S. Guzmán and T. Matos, Class. Quantum Grav. 17 (2000) L9.

[4] J. Magaña, T. Matos, J. Phys. Conf. Ser. 378 (2012) 012012.

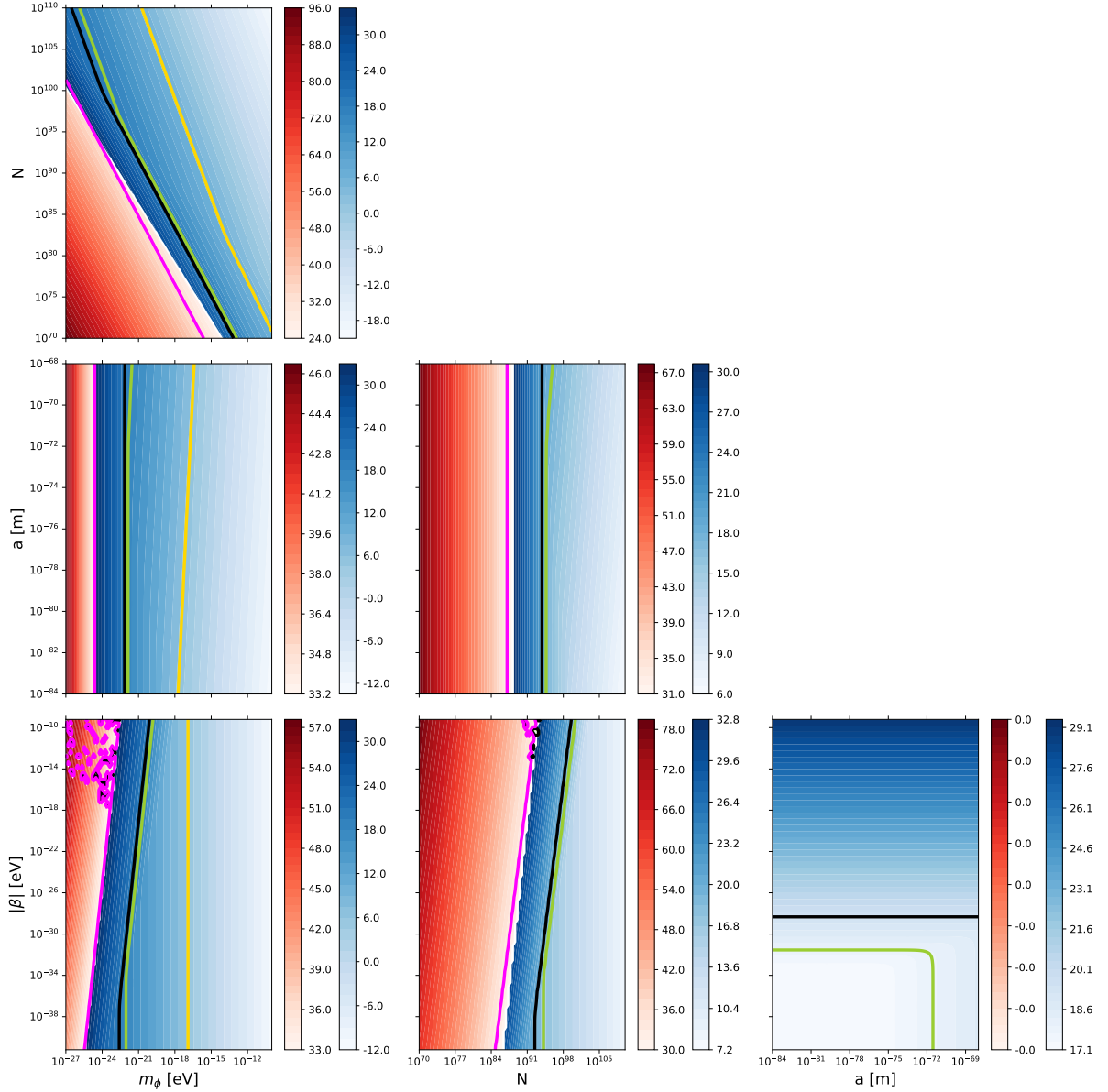


FIG. 6: Triangular plot of the parameter space for a quantum-droplet model, with parameters m_ϕ , a , N , and β fixed to the benchmark values for the Dwarf DM halo system, but for negative values of β , see Table II. The color scheme and description are similar to those in Fig. 1. We have also plotted a magenta isoline for the threshold radii, Eq.(32), for which particle interactions dominate in the system.

- [5] E. Castellanos, J. C. Degollado, C. Lammerzähl, A. Macías and V. Perlick, *J. Cosmol., Astropart. Phys.* 01 (2018) 043.
- [6] E. Castellanos, C. Escamilla–Rivera and J. Mastache, *Int. J. Mod. Phys. D* 29 (2020).
- [7] D. J. Kaup, *Phys. Rev.* 172 (1968) 1331.
- [8] R. Ruffini and S. Bonazzola, *Phys. Rev.* 187 (1969) 1767.
- [9] S. Carignano, L. Lepori, A. Mammarella, M. Mannarelli and G. Pagliaroli, *Eur. Phys. J. A* 53 (2017) 35.
- [10] F. Schunck and E. Mielke, *Class. Quantum Grav.* 20 (2003) R301.
- [11] I. M. Moroz, R. Penrose, and P. Tod, *Class. Quantum Grav.* 15, 2733 (1998).
- [12] L. Visinelli *Int. J. Mod. Phys. D* Vol. 30, Issue 15, No. 2130006 (2021)
- [13] F. Kling and A. Rajaraman, *Phys. Rev. D* 96 (2017) 044039.
- [14] F. Kling and A. Rajaraman, *Phys. Rev. D* 97 (2018) 063012.
- [15] E. Braaten, H. Zhang, *Rev. Mod. Phys.* 91 (2019) 041002.
- [16] M. Alcubierre, et al., *Phys. Rev. D* 107, 045017 (2023).
- [17] C. R. Cabrera, L. Tanzi, J. Sanz, B. Naylor, P. Thomas, P. Cheiney, L. Tarruell, *Science* 359(6373), 301 (2018).
- [18] G. Semeghini, G. Ferioli, L. Masi, C. Mazzinghi, L. Wolswijk, F. Minardi, M. Modugno, G. Modugno, M. Inguscio, M. Fattori, *Phys. Rev. Lett.* 120(23), 235301 (2018)
- [19] P. Cheiney, C.R. Cabrera, J. Sanz, B. Naylor, L. Tanzi, L. Tarruell, *Phys. Rev. Lett.* 120(13), 135301 (2018).
- [20] E. Castellanos, G. Chacón-Acosta and J. Mastache, *Int. J. Mod. Phys. D.* 31, 7, 2250050 (2022).
- [21] H. Kadau, M. Schmitt, M. Wenzel, C. Wink, T. Maier, I. Ferrier-

| | m_ϕ [eV] | N | a [m] | β [eV] | R_0/R_i | E/E_{0i} |
|-------------------------|------------------------|------------------------|------------------------|-------------------------|-----------|-----------------------|
| Sun ^{min} | 8.56×10^{-18} | 3.29×10^{96} | 3.65×10^{-70} | -6.24×10^{-42} | 0.97 | 1.67 |
| Sun | 1.23×10^{-12} | 5.52×10^{76} | 1.00×10^{-68} | -2.80×10^{-19} | 0.92 | 84.39 |
| Sun ^{max} | 5.52×10^{-18} | 1.36×10^{82} | 1.00×10^{-68} | -1.19×10^{-10} | 0.99 | 6.46×10^{47} |
| Dwarf DM ^{min} | 4.72×10^{-25} | 3.20×10^{105} | 2.41×10^{-70} | -6.24×10^{-42} | 0.97 | 1.67 |
| Dwarf DM | 1.44×10^{-22} | 5.24×10^{94} | 7.72×10^{-75} | -1.39×10^{-32} | 0.93 | 68.37 |
| Dwarf DM ^{max} | 1.55×10^{-27} | 6.61×10^{93} | 2.89×10^{-69} | -3.10×10^{-23} | 0.99 | 2.19×10^{69} |
| Cluster ^{min} | 9.02×10^{-27} | 1.00×10^{110} | 4.37×10^{-69} | -8.74×10^{-31} | 1.02 | 1.67 |
| Cluster | 2.17×10^{-26} | 4.04×10^{104} | 6.28×10^{-83} | -1.67×10^{-31} | 1.21 | 76.53 |
| Cluster ^{max} | 1.00×10^{-27} | 4.15×10^{95} | 1.91×10^{-69} | -4.13×10^{-26} | 0.98 | 1.09×10^{58} |

TABLE II: Same description as Table I, but for systems modeled with a negative nonlinear interaction strength, $\beta < 0$. The parameters describing the system and the nomenclature remain the same.

- Barbut, T. Pfau, Nature 530(7589), 194 (2016).
- [22] I. Ferrier-Barbut, H. Kadau, M. Schmitt, M. Wenzel, T. Pfau, Phys. Rev. Lett. 116(21), 215301 (2016).
- [23] L. Chomaz, S. Baier, D. Petter, M.J. Mark, F. Wächtler, L. Santos, F. Ferlaino, Phys. Rev. X 6(4), 041039 (2016).
- [24] M. Schmitt, M. Wenzel, F. Böttcher, I. Ferrier-Barbut, T. Pfau, Nature 539(7628), 259 (2016).
- [25] A.V. Avdeenkov, K.G. Zloshchastiev, J. Phys. B At. Mol. Opt. Phys. 44(19), 195303 (2011).
- [26] Rodríguez-López, O. A., Castellanos, E., J. Low Temp Phys 204, 111–128 (2021). <https://doi.org/10.1007/s10909-021-02601-y>
- [27] S. Vowe, C. Lämmerzahl, M. Krutzik, Phys. Rev. A **101**(4), 043617 (2020)
- [28] I. Bialynicki-Birijla, J. Mycielski, Ann. Phys. **100**, 62-93 (1976).
- [29] C. J. Pethick and H. Smith, Bose-Einstein Condensation in Dilute Gases Cambridge University Press, Cambridge 2004.
- [30] J. Eby et al., Phys. Rev. D 98 (2018) 123013.
- [31] L. Hui, J. P. Ostriker, S. Tremaine and E. Witten, “Ultralight scalars as cosmological dark matter,” Phys. Rev. D **95**, no.4, 043541 (2017) doi:10.1103/PhysRevD.95.043541 [arXiv:1610.08297 [astro-ph.CO]].
- [32] C. C. Bradley, C. A. Sackett, J. J. Tollett and R. G. Hulet, “Evidence of Bose-Einstein Condensation in an Atomic Gas with Attractive Interactions,” Phys. Rev. Lett. **75**, 1687-1690 (1995) doi:10.1103/PhysRevLett.75.1687

Appendix A: Astrophysical objects

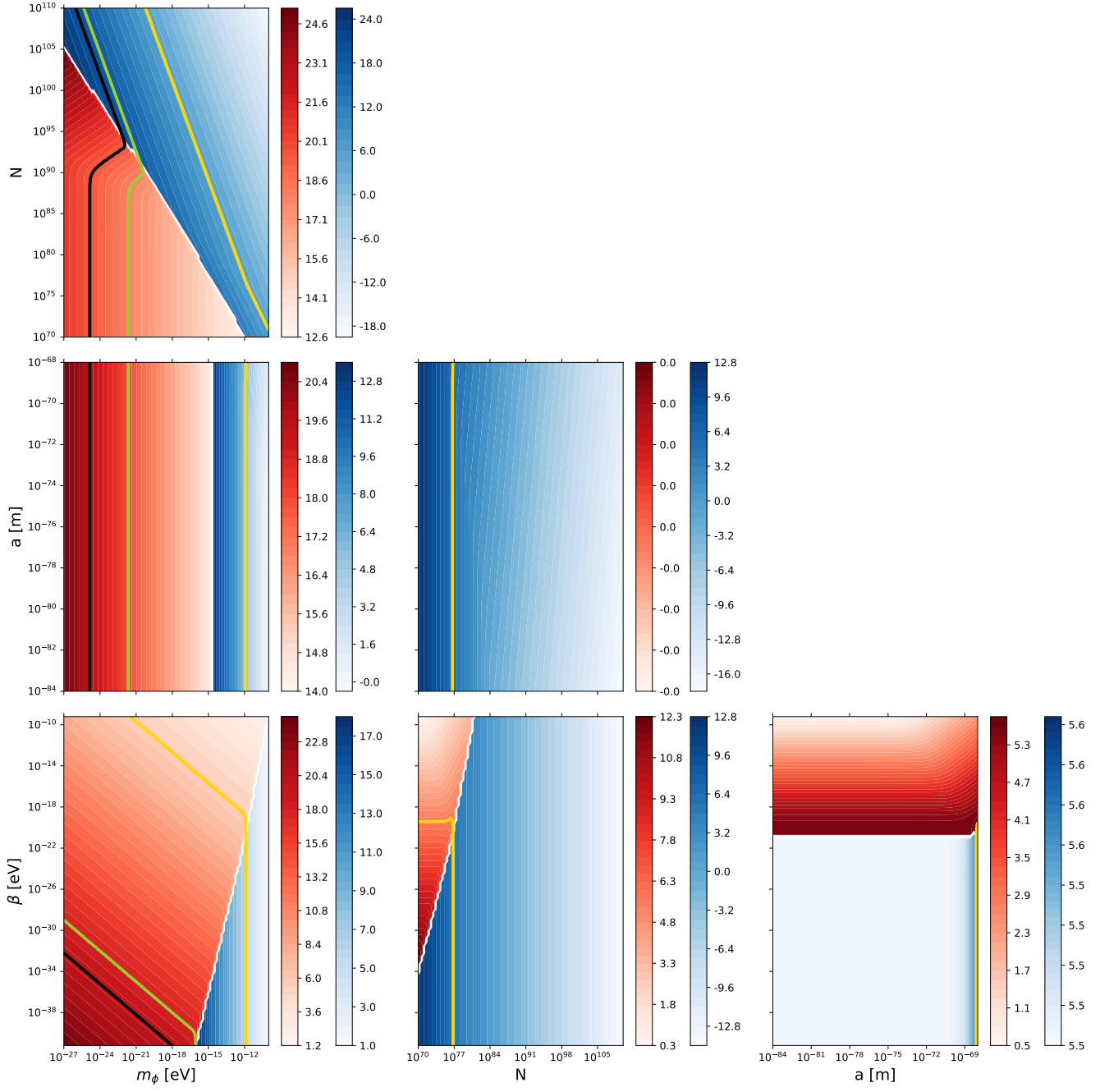


FIG. 7: Parameter space of the Boson star constituted by the parameter m_ϕ , N , a , and β . In red are stable bound in which attractive interactions dominate in the system.

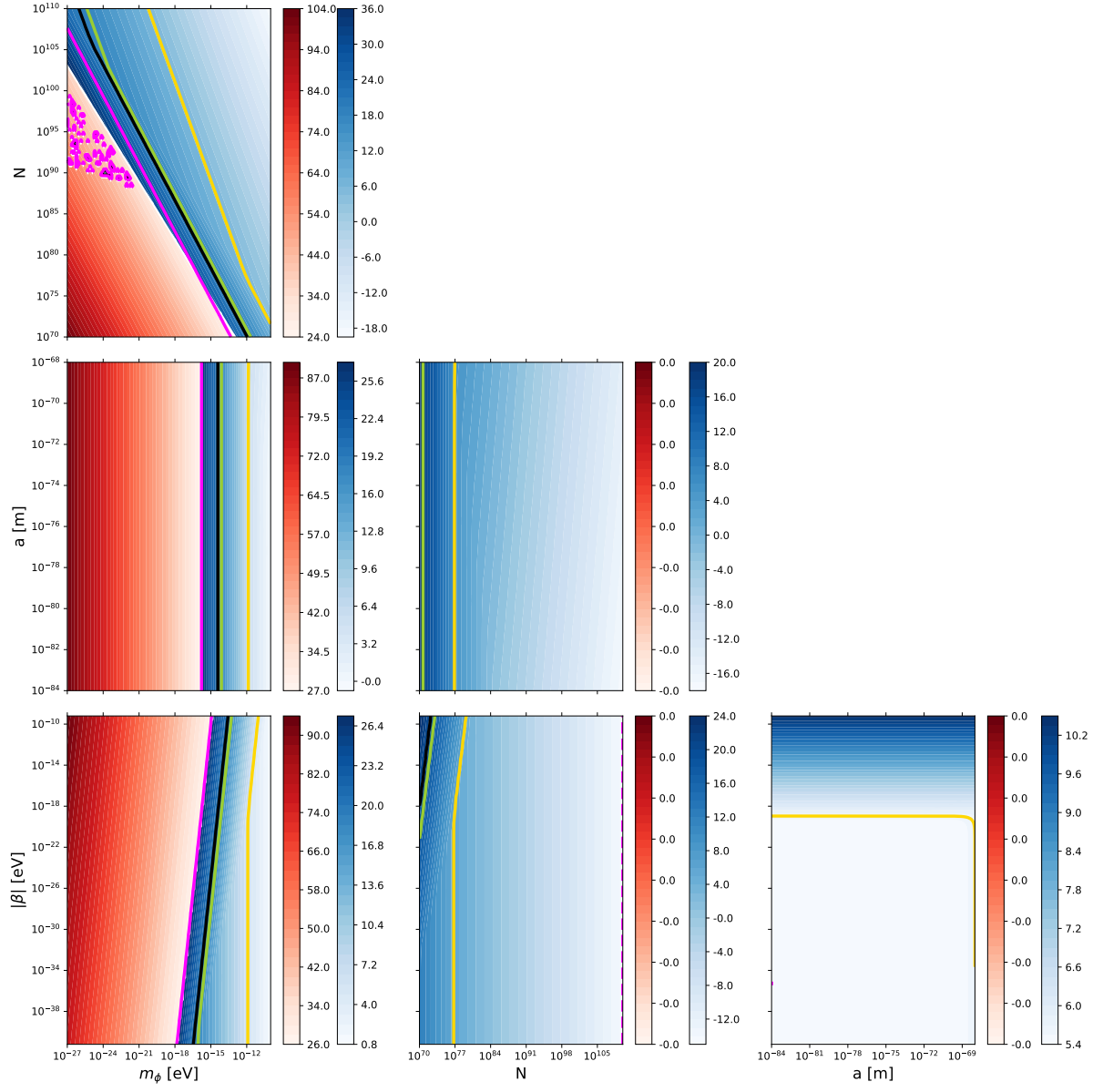


FIG. 8: Top panel: Initial energy value for the perturbed states. Bottom panel: Evolution of the system.

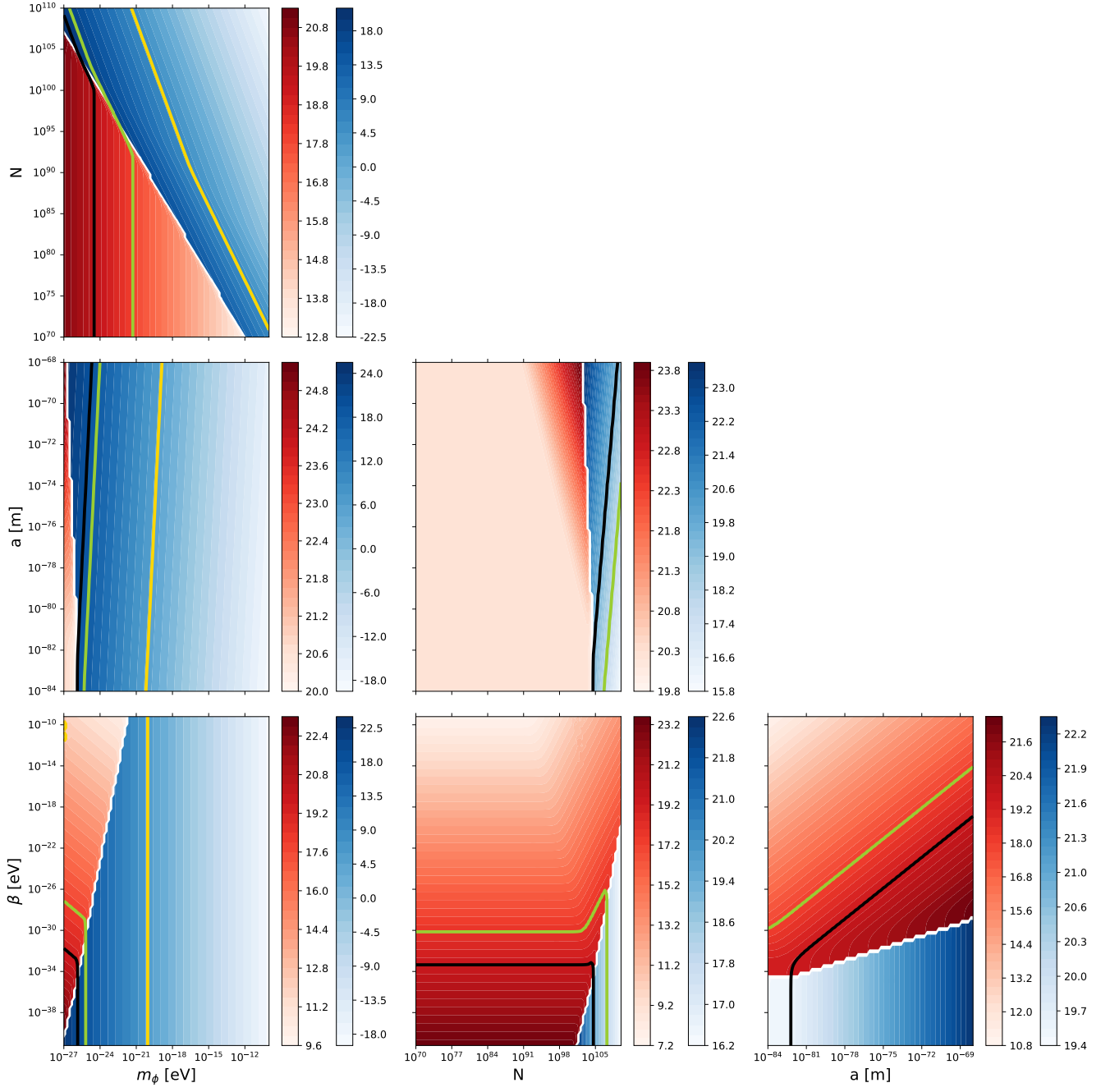


FIG. 9: Parameter space of the Boson star constituted by the parameter m_ϕ , N , a , and β . In red are stable bound in which attractive interactions dominate in the system.

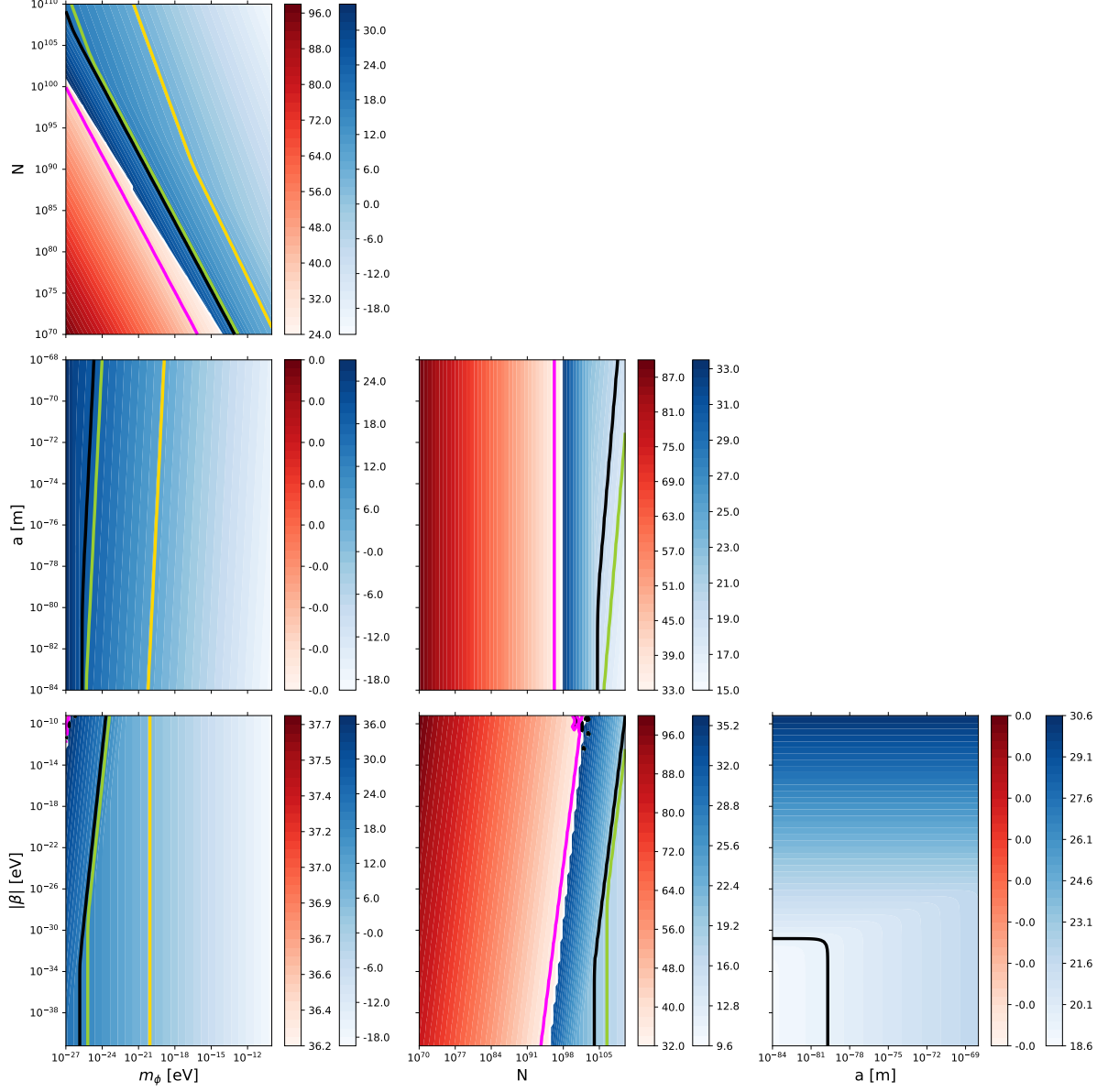


FIG. 10: Top panel: Initial energy value for the perturbed states. Bottom panel: Evolution of the system.